ANTIOXIDANTS & REDOX SIGNALING
Volume 9, Number 3, 2007

DOI: 10.1089/ars.2006.1379

Original Research Communication

Deferoxamine Lowers Tissue Damage After 80% Exchange Transfusion with Polymerized Hemoglobin

PEDRO CABRALES,[1] AMY G. TSAI,[1,2] and MARCOS INTAGLIETTA[1,2]

ABSTRACT

Hemoglobin (Hb) solutions have been proposed as potential substitutes for erythrocytes to maintain oxygen-carrying capacity in situations in which blood is not available. This study investigated systemic and microvascular hemodynamics as well as tissue oxygenation and viability after an 80% exchange transfusion with an oxygen-carrying blood substitute based on polymerized bovine hemoglobin (PBH). Studies were carried in unanesthetized hamsters prepared with a window-chamber model for microcirculation evaluation. Heme iron-mediated injury to the tissue was analyzed by using deferoxamine (an iron chelator), which reduces free iron toxicity. Exchange transfusion led to a significant decrease in hematocrit (Hct) and an increase in plasma Hb, in addition to a significant decrease of arteriolar and venular diameters, flow velocity, and, therefore, microvascular blood flow. Capillary perfusion was severely compromised after exchange, but tissue pO_2 increased above baseline, and oxygen extraction was reduced. Apoptotic and necrotic cells increased significantly after the exchange; however, this effect was only partially due to the toxicity of free iron. Iron therapy decreased the microvascular and oxygenation changes but did not fully reverse the adverse effects. Assessment of tissue viability after exchange suggests that chelation treatment in cases of large exchange transfusions with acellular Hb could be potentially beneficial. *Antioxid. Redox Signal.* 8, 375–384.

INTRODUCTION

Molecular hemoglobin (Hb)-based oxygen carriers (HBOCs) are being developed as blood substitutes and tested in clinical trails (38). In general, HBOCs present potential advantages over erythrocytes for transfusion, including a prolonged shelf life, a lower risk of transfusion reactions, and a faster oxygen uptake (38). However, long-term complications related to the breakdown of the Hb are not well understood. Cell-free Hb binds nitric oxide (NO), causing hypertension after the infusion of most molecular Hb solutions. A consequence of this reaction with NO and other radicals is that Hb is oxidized to methemoglobin (metHb), which is generally more toxic than reduced Hb (3). MetHb, for instance, can release free heme to the endothelium and tissues, sensitizing them to an oxidative reaction via the catalytic properties of the heme, aggravating vascular damage (2).

Metabolism of HBOCs is identical to that of native Hb released when red blood cells (RBCs) are acutely or chronically destroyed (hemolytic anemia, sickle cell anemia, thalassemia, and malaria) (38). Investigators have reported that mild RBC hemolysis after cardiopulmonary bypass saturates transferrin iron-binding capacity, produces iron overload, and compromises endothelial integrity (21, 25). Elevation of total plasma iron has also been correlated with nonsurvival of patients, suggesting that an increased iron mobilization in a deprived transferrin condition (hemodilution) decreases the ability to protect against iron-catalyzed oxidative stress (26). The release of iron from intracellular storage sites, even in small quantities, followed by introduction of molecular oxygen, promotes iron–oxygen interaction, setting the stage for free-radical formation. Earlier experimental studies of ischemia and reoxygenation showed that deferoxamine (DFO) conjugates reduce microvascular injury, suggesting that chelation

[1]La Jolla Bioengineering Institute, La Jolla, California.
[2]Department of Bioengineering, University of California, San Diego, La Jolla, California.

of iron during volume expansion may provide vascular protection (9). Although the literature on iron chelation is extensive, the concept of co-administrating iron chelators at the time of fluid exchange or resuscitation with HBOCs has not been explored.

The variety of HBOC formulations leads to disparate claims about efficacy and ability to oxygenate tissues (7, 36, 38). The first material to gain veterinary approval from the Food and Drug Administration (FDA) in early 1998 was the veterinary product Oxyglobin (Biopure Corporation, Cambridge, MA, U.S.A.). Oxyglobin (polymerized bovine hemoglobin, PBH) is a highly purified bovine Hb, inter- and intramolecularly cross-linked with glutaraldehyde. It is commercially available for oxygen-therapy use in anemic dogs. PBH consists of a heterogeneous mixture of polymeric (~95%) and nonpolymeric (~5%) species ranging in size from 32 to 500 kDa (20). Polymerization with glutaraldehyde is known to alter the oxygen affinity, redox potential, and autoxidation kinetics of human and bovine Hb (1, 13).

The objective of the present study was to understand the potential injury resulting from the breakdown of PBH. It was designed to document, at the microvascular level, the potential damage due to the use of PBH as an HBOC after a large volume-exchange transfusion (80% of the blood volume). The metal chelator DFO was used to evidence the iron-related toxicity and to correlate this to changes in microvascular perfusion.

METHODS

Materials

All chemicals were of analytic grade. DFO was purchased from Sigma Chemical Company (St. Louis, MO). A stock solution was made by dissolving DFO in isotonic saline, purged with an inert gas (N_2), and stored at 4°C. Further dilutions of the stock solution were made before performing the experiments (10 mg/ml). PBH, commercial name Oxyglobin (13.1 g_{Hb}/dl, polymerized bovine hemoglobin in a modified lactated Ringer's solution), was purchased from Biopure Corp. (Boston, MA). PBH solution was stored in deoxygenated conditions at −70°C. Table 1 lists the physical characteristics of the test solutions.

Animal preparation

Investigations were performed by using Golden Syrian hamsters. The hamster window-chamber model is widely used for microvascular studies in the unanesthetized state. The complete surgical technique is described in detail elsewhere (10). The animals were given at least 2 days to recover from window implantation, and then they were anesthetized, and arterial and venous catheters (PE-50; Intramedic, Franklin Lakes, NJ) were implanted in the carotid artery and jugular vein (10, 34). The experiment was performed after at least 24 h but within 48 h of catheter implantation. Animal handling and care were provided by following the procedures outlined in the *Guide for the Care and Use of Laboratory Animals* (National Research Council, 1996). The study was approved by the local Animal Subjects Committee.

TABLE 1. PHYSICAL CHARACTERISTICS OF THE SOLUTION

	PBH Solution
Mean molecular mass (kDa)	180[p] (32–500 kDa)
COP (mm Hg)	38.7*†
Viscosity (cP)	1.8*†
Hb (g/dL)	13.1‡
p50 (mm Hg)	54.2†
n50	1.17†
Hb saturation in room air (%)	72.1 (Ref. 22)
Methemoglobin (%)	<5%‡
Endotoxin (endotoxin units/mL)	<0.05‡
pH	7.8‡

*Shear rate of 160 s^{-1} at 37°C; COP, colloid osmotic pressure at 27°C. p50, pO_2 where 50% of Hb is saturated with O_2. n50, Hill coefficient at 50% saturation.

†Measured parameter. ‡Information from package insert.

Inclusion criteria

Animals were suitable for the experiments if (a) systemic parameters were within normal range, namely heart rate (HR), 340–460 beats/min; mean arterial blood pressure (MAP), 80–120 mm Hg; systemic Hct, 45–52%; and arterial oxygen partial pressure (p_aO_2), 50–72 mm Hg (12); and (b) microscopic examination of the tissue in the chamber observed under ×650 magnification did not reveal signs of edema or bleeding.

Systemic parameters

MAP and HR were recorded continuously (MP 150; Biopac System, Santa Barbara, CA), except during the actual blood exchange. Hct was measured from centrifuged arterial blood samples taken in heparinized capillary tubes (Readacrit; Becton-Dickinson, Parsippany, NJ). Hb content was determined spectrophotometrically from a single drop of blood (B-Hemoglobin; Hemocue, Stockholm, Sweden).

Blood chemistry

Arterial blood was collected in heparinized glass capillaries (0.05 ml) and immediately analyzed for arterial oxygen tension (p_aO_2), arterial carbon dioxide tension (p_aCO_2), and pH (Blood Chemistry Analyzer 248; Bayer, Norwood, MA). Whole blood lactate concentration was measured from 25-µl samples (YSI 1500 SPORT Lactate Analyzer; YSI Incorporated, Yellow Springs, OH).

Measurement of cell-free methemoglobin

Plasma Hb was collected from microhematocrit tubes 2 min after centrifugation, and approximately 50 µl of the RBC-free solution was used. MetHb was determined according to Winterbourn (39). Calibration was ensured by using standard levels at 5.2%, 2.6%, and 1.2% metHb (RNA Medical, CO-Oximeter Control; Bayer Diagnostics, Medfield, MA). In normal conditions, the concentration of cell-free Hb

in the hamster is lower than 0.08 g/dl, and cell-free metHb can not be detected.

Functional capillary density (FCD)

Functional capillaries, defined as those capillary segments that have RBC transit of at least a single RBC in a 30-s period, were assessed in 10 successive microscopic fields, totaling a region of 0.46 mm^2. Observation of the fields was done systematically by displacing the microscopic field of view by a field width in 10 successive steps in the lateral direction. The first field was chosen by a distinctive anatomic landmark, easily and quickly to reestablish the same fields at each observation time point. Each field had between five and 10 capillary segments with RBC flow. FCD (cm^{-1}), total length of RBC perfused capillaries divided by the area of the microscopic field of view, was evaluated by measuring and adding the length of capillaries that had RBC transit in the field of view. The relative change in FCD from baseline levels after intervention is indicative of the extent of capillary perfusion.

Microhemodynamics

Arteriolar and venular blood-flow velocities were measured online by using the photodiode cross-correlation method (19) (Photo Diode/Velocity Tracker Model 102B; Vista Electronics, San Diego, CA). The measured centerline velocity (V) was corrected according to vessel size to obtain the mean RBC velocity. A video image-shearing method was used to measure vessel diameter D (16). Blood flow Q was calculated from the measured values as $Q = V \times \pi(D/2)^2$. Changes in arteriolar and venular diameter from baseline were used as indicators of a change in vascular tone.

Microvascular pO_2 Distribution

High-resolution microvascular pO_2 measurements were made by using phosphorescence-quenching microscopy (PQM) (32). This method for measuring oxygen levels is based on the oxygen-dependent quenching of phosphorescence emitted by albumin-bound metalloporphyrin complex after pulsed-light excitation. The phosphorescence decay curves were converted to oxygen tensions by using a fluorescence decay curve fitter (model 802; Vista Electronics, Ramona, CA) (18). Animals received a slow intravenous injection of 15 mg/kg body weight at a concentration of 10.1 mg/ml of a palladium-meso-tetra(4-carboxyphenyl) porphyrin (PdTCPP; Porphyrin Products, Inc., Logan, UT). The dye was allowed to circulate for 10 min before pO_2 measurements (18, 32).

In our system, intravascular measurements are made by placing an optical rectangular window (5 x 15 μm) within the vessel of interest, with the longest side of the rectangle slit positioned parallel to the vessel wall. Tissue pO_2 is measured in regions void of large vessels within intercapillary spaces (10 x 10 μm) (33).

Oxygen delivery and extraction

Calculations of oxygen delivery, $O_{2\ delivery}$, and extraction, $O_{2\ extraction}$ (6), are made by using equations 1 and 2:

$$O_{2\ delivery} = [(RBC_{Hb}\ \gamma\ S_A\ \%) + (PBH_{Hb}\ \gamma\ \&\#348;_A\ \%) + (1 - Hct)\ \alpha\ pO_{2A}]\ Q \quad [1]$$

$$O_{2\ extraction} = [(RBC_{Hb}\ \gamma\ S_{A\text{-}V}\ \%) + (PBH_{Hb}\ \gamma\ \&\#348;_{A\text{-}V}\ \%) + (1 - Hct)\ \alpha\ pO_{2A\text{-}V}]\ Q \quad [2]$$

where RBC_{Hb} and PBH_{Hb} are the Hb in RBCs and PBH, γ is the oxygen-carrying capacity of Hb (1.34 ml O_2/g_{Hb}), $S_A\%$ and $\hat{S}\%$ are the arteriolar oxygen saturation for RBC and PBH, $(1 - Hct)$ is the blood fraction of plasma, α is the solubility of oxygen in plasma (3.14×10^{-3} ml O_2/dl × mm Hg), pO_{2A} is the arteriolar partial pressure of oxygen, Q is the microvascular flow relative to baseline, and the subscript A-V indicates the difference between arterioles and venules.

Visualization of cell death in vivo

Equal volumes of annexin V (Alexafluor 488 conjugate, catalog no. A-13201; Molecular Probes, Eugene, OR) and propidium iodide (0.2 mg/ml; Molecular Probes) were mixed, and 140 μl of the mixture was injected 30 min before visualization by intravital microscopy (40). Imaging of labeled cells was performed at 8 h after the exchange transfusion. Microscopic images were obtained with a low-light video camera (ORCA 9247; Hamamatsu, Tokyo, Japan) and recorded at 5 frames per second and1,344 × 1,024 pixels per frame. Single- and double-labeled cells were counted in the skin-fold window, and the percentages of cells labeled with annexin V and/or propidium iodide were calculated at different time points. Data are given as the average of fluorescent cells counted in 40 selected visual fields (210 × 160 μm) of tissue and endothelial vessel wall. Sebaceous glands and hair follicles were identified and excluded from the cell counts because of their consistently high necrosis and apoptosis rates.

TUNEL tissue viability

The occurrence of apoptosis was assessed with the terminal transferase–mediated dUTP nick end-labeling (TUNEL) assay (In Situ Cell Death Detection Kit, TMR fluorescein; Roche Diagnostics, Alameda, CA). All steps were performed according to the supplier's instructions. Sections of green-labeled cells (excitation wavelength, 450–500 nm; detection, 515–565 nm) were immediately examined with a fluorescence microscope (BX51WI; Olympus, New Hyde Park, NY; objectives, ×40, ×60 LUMPFL-WIR; numerical aperture, 0.8; Olympus).

Acute isovolemic hemodilution

Progressive hemodilution was accomplished by a single-step isovolemic exchange. In brief, the volume of the exchange transfusion was calculated as a percentage of the blood volume, estimated as 7% of body weight. PBH was infused into the jugular vein catheter passing through an in-line 0.2-μm syringe filter (rate of 100 μl/min). Blood was simultaneously withdrawn by a dual-syringe pump ("33" syringe pump; Harvard Apparatus, Inc., Holliston, MA) at the same rate from the carotid artery catheter. This slow rate of exchange provided a stable cardiac output, heart rate, and MAP during the procedure.

Deferoxamine treatment

Deferoxamine (DFO, Desferal) at a dose of 150 μmol/kg, i.v., was given 5 min before and 10 min after the PBH exchange transfusion, and 1 h later, the dose was repeated.

Experimental groups

Animals were randomly divided into two experimental groups by sorting a set of numbers produced in a random-ordering scheme. Groups were labeled ***PBH*** (n = 10, animal exchange with PBH without DFO therapy) and ***PBH-DFO*** (n = 10, animal exchange with PBH with DFO therapy). Each study group was divided into two for the analysis of (a) microhemodynamics/tissue oxygenation (n = 5), and (b) tissue-viability studies (n = 5). This division was used to reduce artifacts induced by the phosphorescence quenching technique used to measure oxygen (11). A group that did not undergo the hemodilution protocol served as control for this study.

Experimental setup and procedure

The unanesthetized animal was placed in a restraining tube with a longitudinal slit from which the window chamber protruded. Animals were given 30 min to adjust to the tube environment before baseline parameters were measured. The conscious animal was secured to the microscope stage of a transillumination intravital microscope (BX51WI; Olympus). The tissue image was projected onto a charge-coupled device camera (COHU 4815; San Diego, CA). Measurements were carried out by using a ×40 (LUMPFL-WIR, numerical aperture 0.8, Olympus) water-immersion objective. Detection of RBC passage was enhanced by increasing contrast between RBCs and tissue by using a 420-nm bandpass filter.

Fields of observation and vessels were chosen for study at locations in the tissue where the vessels were in sharp focus. Detailed mappings were made of the chamber vasculature to record the vessel location and ensure that the same microvessels were studied throughout the experiment. Systemic and microcirculatory parameters were studied in each animal at baseline as well as 1, 6, and 8 h after isovolemic hemodilution with PBH. Microvascular pO_2 distribution was measured at 1 and 6 h after isovolemic hemodilution with PBH. Tissue viability was assessed 8 h after isovolemic hemodilution with PBH.

Data analysis

Results are presented as mean ± standard deviation. Data within each group were analyzed by using analysis of variance for repeated measurements (ANOVA, Kruskal–Wallis test). When appropriate, *post hoc* analyses were performed with the Dunn multiple comparison test. Microhemodynamic measurements were compared with baseline levels obtained before the experimental procedure. Microhemodynamic data are presented as absolute values and ratios relative to baseline values. A ratio of 1.0 signifies no change from baseline, whereas lower and higher ratios are indicative of changes proportionately lower and higher than baseline (*i.e.*, 1.5 would mean a 50% increase from the baseline level). The same vessels and functional capillary fields were followed so that direct comparisons with their baseline levels could be performed, allowing more robust statistics for small sample populations. All statistics were calculated by using GraphPad Prism 4.01 (GraphPad Software, Inc., San Diego, CA). Changes were considered statistically significant if $p < 0.05$.

RESULTS

Studies were completed in 24 preparations; four animals did not undergo the hemodilution protocol and were used to establish control levels for apoptosis/necrosis. Twenty animals (55–65 g) were used (exchange transfusion, PBH, n = 10 and PBH-DFO, n =10) to characterize microvascular and systemic events at each time point after exchange transfusion (1, 6, and 8 h). Each animal was studied at baseline (BL) and at the specified time point (1, 6, and 8 h). Oxygen measurements were performed on five of the animals in each group at 1 and 6 h, by using a single dose of porphyrin for each time point. In animals not used for oxygen measurements, tissue viability was assessed at 8 h after exchange (tissue viability subgroup, PBH, n = 5, and PBH-DFO, n = 5). Animals were placed in their normal environment with available food and water between observation time points.

Systemic and blood gas parameters

Systemic, blood gas parameters, Hct, and Hb for each group are presented in Table 2. Heart rate at 1 h after exchange transfusion with PBH was not different from baseline and did not change after 6 and 8 h. MAP was statistically higher at 1, 6, and 8 h after exchange transfusion. The comparatively low p_aO_2 and high p_aCO_2 values of these animals are a consequence of their adaptation to a fossorial environment. p_aCO_2 remained statistically significantly decreased from baseline throughout the experimental procedure, although no evidence was found of changes in the breathing pattern. A statistical increase in pO_2 was noted 1 and 6 h after exchange with PBH, but it was not different from baseline at 8 h. Blood pH was not statistically changed. Lactate levels showed a statistically significant increase after exchange transfusion, except after 6 and 8 h in the DFO-treated group.

The concentration of HCO_3 was not determined because the gas analyzer (Blood Chemistry Analyzer 248; Bayer, Norwood, MA, U.S.A.) used in this study uses pH, pO_2, and pCO_2 values to calculate BE and HCO_3. The Henderson-Hasselbach equation is then used to calculate HCO_3 values. However, this calculation does not take into account pertinent experimental conditions, particularly the large amount of cell-free Hb, which acts as a buffer, uncoupling the calculated parameters from their actual value. In view of this problem, we do not report calculated parameters such as HCO_3 and BE.

Microhemodynamics

At 1 h after exchange, arteriolar (A) and venular (V) diameters were statistically different from baseline in the PBH and PBH-DFO groups. Arteriolar diameters did not fully recover at 6 or 8 h, but venular diameters recovered after 6 and 8 h. Combining diameter and flow-velocity data allowed us to calculate arteriolar and venular flows, as shown in Fig. 1, indicating that at 1 h after exchange, arte-

TABLE 2. LABORATORY PARAMETERS BEFORE AND AFTER BLOOD EXCHANGE

		After exchange					
		PBH			*PBH-DFO*		
	Baseline	*1 h*	*6 h*	*8 h*	*1 h*	*6 h*	*8 h*
Hct (%)	48.9 ± 0.8	18.7 ± 0.7†	20.1 ± 0.6†	20.7 ± 0.8†	19.0 ± 0.8†	20.4 ± 0.7†	20.3 ± 0.9†
Hb (g/dl)							
Whole Blood	14.8 ± 0.6	11.2 ± 0.3†	10.6 ± 0.4†	10.1 ± 0.6†	11.4 ± 0.3†	10.8 ± 0.3†	10.2 ± 0.5†
Plasma		6.2 ± 0.4	4.6 ± 0.3§	4..0 ± 0.4§	6.3 ± 0.3	4.6 ± 0.2§	4.2 ± 0.4§
Plasma MetHb, %		9 ± 3	6 ± 2§	5 ± 2§	7 ± 2	5 ± 2	4 ± 2§
MAP (mm Hg)	104 ± 8	121 ± 5†	119 ± 7†	120 ± 9†	120 ± 6†	117 ± 6†	115 ± 7†
Heart Rate	419 ± 30	388 ± 35	399 ± 26	405 ± 34	397 ± 33	409 ± 28	401 ± 36
paO_2 (mm Hg)	60 ± 5	72 ± 7†	68 ± 5†	66 ± 8	75 ± 6†	72 ± 5†*	70 ± 7†
$paCO_2$ (mm Hg)	56 ± 6	48 ± 6†	44 ± 5†	47 ± 6†	47 ± 5†	44 ± 6†	48 ± 7†
Arterial pH	7.36 ± 0.02	7.38 ± 0.03	7.37 ± 0.03	7.38 ± 0.02	7.37 ± 0.04	7.38 ± 0.03	7.37 ± 0.03
Lactate (mmol)	1.9 ± 0.3	3.1 ± 0.5†	2.8 ± 0.6†	2.7 ± 0.7†	2.9 ± 0.5†	2.3 ± 0.6	2.0 ± 0.4

Values are means ± SD. Baseline included all the animals in the study. No significant differences were detected between the Baseline values of each group. Hct, systemic hematocrit (normal range 45–52%); Hb, hemoglobin content of blood (normal range 12–16 g/dl); MAP, mean arterial blood pressure (normal range 80–120 mm Hg); paO_2, arterial partial O_2 pressure (50–72 mm Hg); $paCO_2$, arterial partial CO_2 pressure (48–62 mm Hg); lactate (normal range 1.5–2.5 mmol). †$p < 0.05$ compared to baseline; §$p < 0.05$ compared to 1h within the group; *$p < 0.05$ compared to time point between groups.

riolar and venular flows were reduced from baseline. Flows were lower at 6 h after exchange and remained lower at 8 h. Microcirculation parameters were improved in the group of animals treated with DFO, but the differences were not statically significant at any time point (p value in the range 0.12–0.21).

Functional capillary density

FCD was reduced at 1, 6, and 8 h after exchange transfusion for PBH (1 h: 0.68 ± 0.09; 6 h: 0.69 ± 0.08; 8 h: 0.71 ± 0.09 relative to baseline; $p < 0.05$) and PBH-DFO (1 h: 0.64 ± 0.11; 6 h: 0.73 ± 0.07; 8 h: 0. 0.81 ± 0.08 relative to baseline; $p < 0.05$). At 8 h after exchange transfusion, PBH FCD was significantly lower than PBH-DFO ($p < 0.05$).

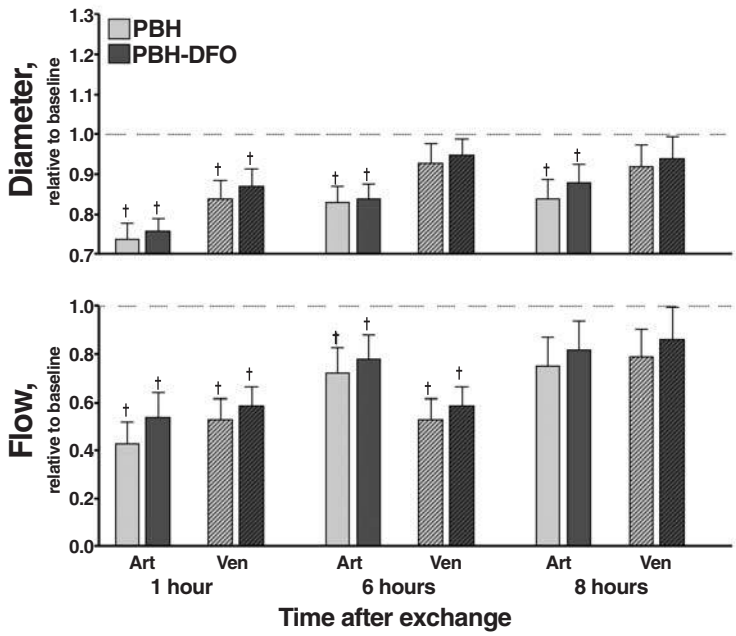

FIG. 1. Relative changes to baseline in arteriolar and venular hemodynamics at 1, 6, and 8 h after exchange transfusion with PBH. Black (PBH), untreated with DFO; Gray, (DFO-PBH), treated with DFO (†, $p < 0.05$ compared with baseline). Diameters (μm, mean ± SD) in each animal group were as follows: Baseline (arterioles (A): 54.5 ± 5.1, $n = 100$, venules (V): 57.4 ± 6.4, $n = 98$); 1 h after exchange (PBH, A: 42.6 ± 6.8, $n = 50$, V: 48.9 ± 8.1, $n = 49$; DFO-PBH, A: 43.5 ± 5.5, $n = 50$, V: 49.4 ± 6.4, $n = 49$); 6 h after exchange (PBH, A: 45.1 ± 7.2, V: 53.1 ± 7.1; DFO-PBH, A: 46.7 ± 7.4, V: 54.2 ± 7.9); 8 h after exchange (PBH, A: 47.6 ± 7.0, V: 50.6 ± 6.6; DFO-PBH, A: 47.9 ± 7.2, V: 51.3 ± 6.5). n, Number of vessels studied. RBC velocities (mm/s, mean ± SD) in each animal group were as follows: Baseline (A: 4.8 ± 1.8, V: 3.2 ± 0.7); 1 h after exchange (PBH, A: 4.2 ± 2.8, V: 2.8 ± 1.2; DFO-PBH, A: 5.4 ± 2.3, V: 2.7 ± 0.9); 6 h after exchange (PBH, A: 5.4 ± 2.5, V: 3.1 ± 1.0; DFO-PBH, A: 5.6 ± 2.0, V: 3.2 ± 0.9); 8 h after exchange (PBH, A: 5.3 ± 2.2, V: 3.4 ± 1.5; DFO-PBH, A: 5.2 ± 2.1, V: 3.6 ± 1.2). Flow (nl/s, mean ± SD) in each animal group were as follows: baseline (A: 12.2 ± 3.8, V: 8.7 ± 2.6); 1 h after exchange (PBH, A: 5.1 ± 3.3, V: 4.9 ± 2.5; DFO-PBH, A: 6.9 ± 3.0, V: 5.1 ± 2.0); 6 h after exchange (PBH, A: 8.4 ± 4.1, V: 3.7 ± 2.6; DFO-PBH, A: 9.0 ± 3.8, V: 3.4 ± 2.6); 8 h after exchange (PBH, A: 9.0 ± 4.0, V: 6.7 ± 2.8; DFO-PBH, A: 9.3 ± 4.0, V: 7.5 ± 2.7).

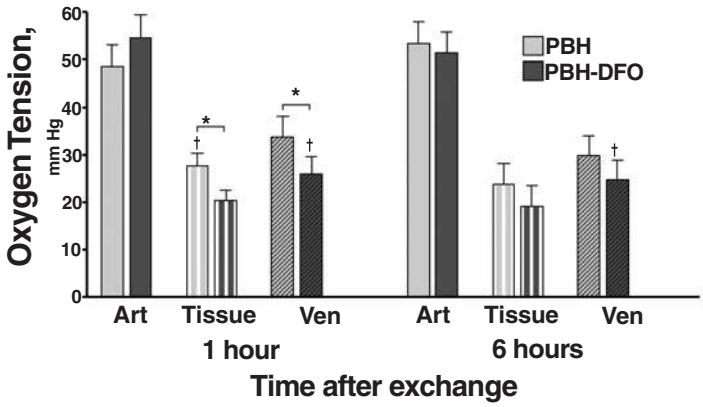

FIG. 2. Intravascular and tissue partial oxygen pressure at 1 and 6 h after exchange transfusion. White, baseline (Control); black (PBH), untreated with DFO; gray, (DFO-PBH), treated with DFO. (†, $p < 0.05$ compared with baseline). Tissue pO_2 attained at 1 h after exchange for PBH was statistically greater than baseline. Intravascular pO_2 (mm Hg, mean ± SD) values for control (no exchange transfusion, baseline conditions) were as follows: arterioles: 51.5 ± 4.3, $n = 32$; venules: 34.7 ± 3.4, $n = 38$; tissue: 22.3 ± 3.2, $n = 34$).

Microvascular oxygen distribution

Arteriolar oxygen tensions after exchange transfusion at 1 and 6 h were not significantly different from baseline (Fig. 2). Venular pO_2 for PBH was maintained at 1 h after exchange and decreased at 6 h. Venular pO_2 for PBH-DFO after 1 and 6 h was significantly lower than baseline. Tissue pO_2 for PBH at 1 h after the exchange was significantly higher than baseline. Tissue pO_2 for PBH at 6 h and for PBH-DFO at 1 and 6 h were no different from baseline.

Arteriolar wall gradients were determined from the difference between intravascular and perivascular po_2 measurements performed across the vessel walls. This parameter has been shown to be directly related to the rate of oxygen consumption of the vessel wall (33). The vessel-wall gradient in arterioles at baseline conditions was 16 ± 2 mm Hg ($n = 22$). This value decreased 1 h after exchange to 10 ± 3 mm Hg ($n = 22$; $p < 0.05$) for PBH and to 15 ± 3 mm Hg ($n = 22$; $p = 0.12$) for PBH-DFO, remained reduced at 6 h for PBH to 12 ± 3 mm Hg ($n = 22$; $p < 0.05$), and increased for PBH-DFO to 18 ± 2 mm Hg ($n = 22$; $p < 0.05$), respectively.

Cell-free methemoglobin

MetHb in the PBH solution before injection was 2 ± 1%, $n = 5$. At 1 h after exchange, oxidation cell-free Hb increased significantly, and metHb was 9 ± 3% for PBH and 7 ± 2% for PBH-DFO. Six hours after exchange transfusion, metHb decreased to 6 ± 2% for PBH and 5 ± 2% for PBH-DFO, and was 5 ± 2% for PBH and 4 ± 2% for PBH-DFO at 8 h after the exchange transfusion.

Tissue oxygen delivery and extraction

Calculations of oxygen delivery showed that the lowest oxygen delivery and extraction was at 1 h after exchange for the PBH and remained low after 6 h (Fig. 3). For PBH-DFO, oxygen delivery was statistically significantly lower than baseline at 1 and 6 h, and no different from PBH. Oxygen extraction for PBH-DFO was not different from baseline and significantly higher than PBH at 1 h. Baseline oxygen delivery and extraction were 7.0 ± 1.2 ml O_2/dl_{blood} and 3.2 ± 0.8 ml O_2/dl_{blood}, respectively, with an extraction ratio of 42%, which matches previous reports for the hamster window model (6, 34).

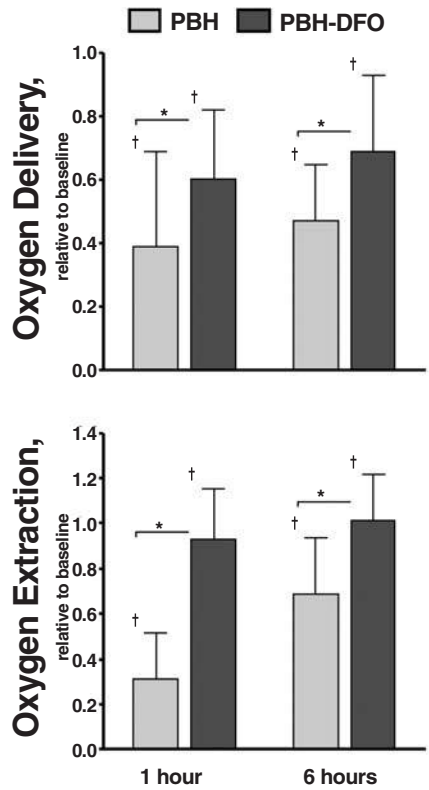

FIG. 3. Arterial oxygen delivery and extraction at baseline, 1 and 8 h after exchange transfusion. Black (PBH), untreated with DFO; gray, (DFO-PBH), treated with DFO. (†, $p <$ 0.05 compared with baseline). Calculations of global oxygen transport are not directly measurable in our model; however, the changes relative to baseline can be calculated by using the measured parameters. These calculations can be identified as those presented without standard deviations to focus on their tendencies rather than on the variability of the measurement. Extraction ratio 1 h after for PBH was 28% and for DFO-PBH was 47%; 6 h after the extraction ratio for PBH was 53% and for DFO-PBH was 58%.

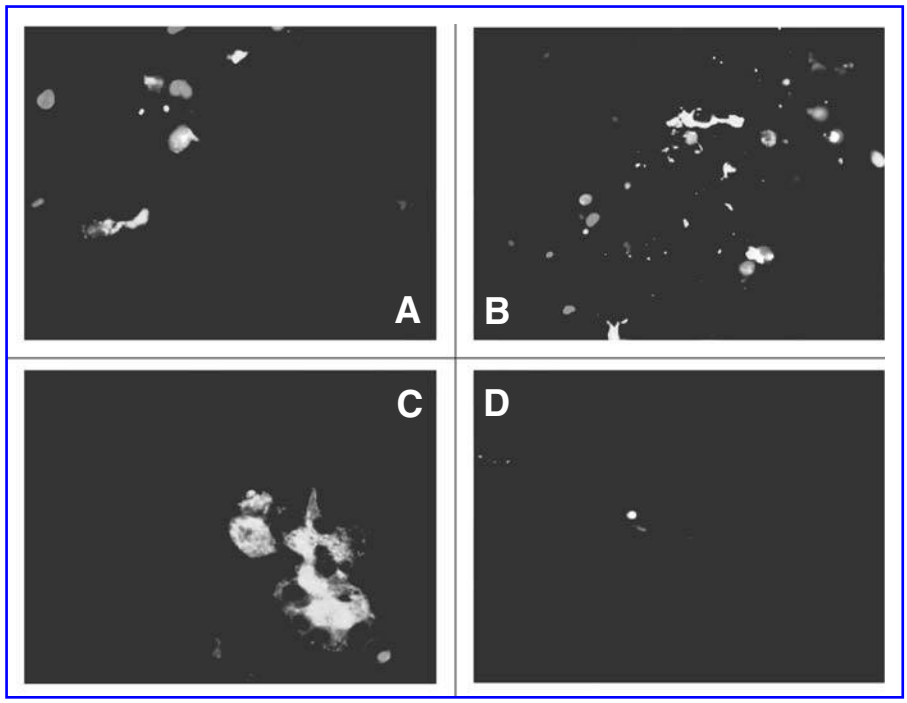

FIG. 4. In vivo labeled cells with annexin V and/or propidium iodide (PI) in the hamster window model. Cell membranes were stained with annexin V, and nuclei were stained with PI. (**A–D**) Images of stained fields 8 h after exchange transfusion with PBH. (**A**) An equal distribution of apoptotic, early apoptotic and necrotic tissue. [Green stain (presented as light gray) is annexin V, and red (presented as dark gray) is PI.] (**B**) High number of necrotic cells and ischemic zones as a consequence of vasoconstriction. (**C**) Highly apoptotic area. (**D**) Apoptotic endothelial cells.

Tissue viability

Annexin V and PI staining for apoptosis and necrosis were assessed by intravital microscopy (Fig. 4). Annexin V labels only the cell membrane, whereas PI stains the nucleus. Labeled cells by annexin V or PI at control (nonhemodiluted) were <2% of the observed cells. The majority of control labeled cells were necrotic, probably as a consequence of the surgical procedure required for window implantation (Fig. 4). Cells stained only with annexin V (annexin V^+; PI^-; early apoptotic) and those stained with both annexin V and PI (annexin V^+; PI^+, apoptotic) were occasionally observed in the control group. PBH at 8 h after exchange caused a significant increase in the total of labeled cells relative to baseline, which were mostly apoptotic (annexin V^+; PI^+) and early apoptotic (annexin V^+; PI^-; necrotic cells). In the PBH-DFO group at 8 h after the exchange, the total of labeled cells was increased significantly from control, but was significantly lower than with the PBH group. PBH-DFO produced an almost even distribution of apoptotic, early apoptotic, and necrotic cells (Fig. 5). *Ex vivo* TUNEL staining on the hamster window tissue

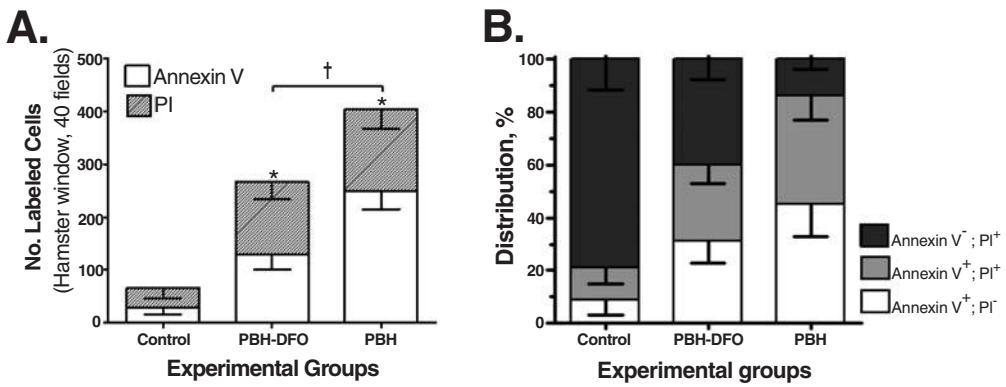

FIG. 5. (A) Total amount of labeled cells in the hamster window. (**B**) Distribution of labeled cells. Five hamster windows were used in each group, 40 fields in each window (reported numbers are for the hamster window). *$p < 0.05$ compared with control; †$p < 0.05$. Control group did not undergo exchange transfusion. PBH and PBH-DFO (with iron chelation therapy) were exchange transfused 80% of the BV with Oxyglobin (Biopure Corporation, Cambridge, MA, U.S.A.). Cells stained only with annexin V (annexin V^+/PI^-; early apoptotic) and stained with both annexin V and PI (annexin V^+/PI^+; apoptotic) were occasionally observed in the control group (annexin V, 27.8 ± 12.3; PI, 37.2 ± 19.6). After exchange transfusion with PBH, the total number of labeled cells increased, for the DFO-treated group (PBH-DFO, annexin V, 128.0 ± 26.3; PI, 138.2 ± 32.0) and untreated (PBH, annexin V, 249.5 ± 34.1; PI, 155.2 ± 36.7).

at 8 h confirmed the result obtained *in vivo* with annexin V and PI.

DISCUSSION

The principal finding of this study is that exchange transfusion with PBH to maintain oxygen-carrying capacity causes a significant loss of tissue viability, as shown by the increase in apoptotic and necrotic cells. The significant number of dead cells should be the cause of the high tissue oxygen levels because the tissue metabolic rate is reduced. DFO treatment partially lowered the extent of cell death, suggesting that other factors are involved, such as loss in microvascular perfusion; thus, cell death should be only partially due to the toxicity of free iron. Tissue viability appeared to be compromised after exchange with PBH, independent of DFO treatment. These phenomena are probably due to oxidative stress, which induces cellular responses ranging from temporary arrest and adaptation to permanent arrest, as shown by the apoptosis and necrosis found in the present study. DFO treatment reduced, but did not eliminate, tissue damage. Our data suggest that PBH may induce some direct or indirect DNA damage, whereas the possibility remains that intracellular oxidative stress induces cell-cycle arrest (8).

The 80% exchange transfusion used in this study is an unusual intervention that, in practice, may occur only as a consequence of uncontrollable bleeding. It is possible that lesser levels of exchange may reduce the toxicity; however, no evidence exists for the existence of a mechanism that becomes inactivated by the high dosage of PBH, causing this to be become toxic only after a specific dosage threshold is reached. More likely, the toxicity effects are gradual and proportional to the concentration of PBH in blood. Therefore, these results suggest that an upper limit may exist to the concentration of PBH that can be safely tolerated in blood.

The massive exchange of blood with PBH may cause metabolic disturbances such as metabolic acidosis. However, pH does not change significantly, and, therefore, the measured changes in pCO_2 and lactate may be due to inherent noise in the data from the large concentration of cell free Hb in blood.

Double staining (annexin V, PI) provided real-time images of the apoptotic and necrotic cells. Apoptosis is an ongoing process, so that cells stained with annexin V should not be kept for a prolonged time before measurement. Cells that still maintain membrane integrity for longer incubation times may become positive for PI, because this dye will slowly enter intact cells. Analysis of cells was performed 10–15 min after incubation.

Our findings are consistent with the possibility that the presence of PBH in the circulation causes a significant decrease in oxygen consumption, which results in more oxygen being available in the tissue, leading to higher tissue pO_2. The latter could, in part, be due to the low affinity of PBH, which favors oxygen unloading, as shown by Page *et al.* (24). However, other factors must be present because the total amount of oxygen delivered and consumed is decreased. The parameter that characterizes oxygen consumption by the microvascular wall is the oxygen gradient measured across this structure (33, 35). If only vessel-wall oxygen metabolism was affected by molecular Hb, oxygen requirements would be ~70% lower. However, our results show that tissue oxygen release was reduced to 30% of baseline, indicating a reduction of oxygen consumption by the parenchyma.

Deferoxamine (DFO) has remained the only effective and safe treatment of iron overload (28), which reduces the organism's iron burden and thus iron-related morbidity and mortality (15). A number of studies have used DFO to examine the role of transition metals such as free ferric iron (not heme-bound forms) in the mechanism of oxidative stress. DFO is able to bind transition metals, reducing and/or inhibiting their catalytic activity, which lowers the effects due to oxidative stress. Oxidative stress can be initiated by free iron, and under such circumstances, DFO is an effective inhibitor; however, DFO can also directly affect oxidative reactions. For example, DFO can act as a substrate for peroxidases and a scavenger of radicals (22). It can also act as an electron donor (37) and inhibit the enhanced pro-oxidant activity of myoglobin and most likely Hb (27). Hamster models have been used to study DFO because of the similarities between human and hamster iron metabolism in terms of plasma stability and metabolites formed (31).

The present study shows that PBH causes apoptotic cell death and that a partial reduction of the phenomenon occurs after the administration of DFO, whose iron-binding capacity gives it a considerable antioxidant potential to inhibit oxygen radical formation driven by iron (14). The origin of the chelatable iron present in our experiments should be entirely due to Hb released from PBH, an effect magnified when PBH turns into MetHb, in which heme is more likely to be released (4, 5, 17). It should be noted that iron released from Hb results from spontaneous and chemically (hydrogen peroxide) induced oxidation of Hb, which ultimately results in heme degradation. PBH has been shown to be more resistant to oxidative damage caused by these reactions than are other HBOCs, and it produces consequently far less heme degradation products and iron (23).

Even though PBH caused significantly lower levels of tissue oxygen consumption 1 h after exchange, we did not find any evidence for global tissue hypoxia when compared with conditions before exchange transfusion. Arterial lactate values were increased but remained within the physiologic range for hamsters. The combined analysis of pH and lactate indicates that lactic acidosis may be present because of the decrease in perfusion and oxygen delivery resulting from the exchange with PBH. PBH is a vasoactive material that scavenges, and the disruption of the NO balance could also affect mitochondria respiration, enzymes, and permeability

The decrease in oxygen delivery is not attributable to a deficit in oxygen-carrying capacity, because the same amount of Hb in RBCs, in the absence of PBH, provides for normal tissue oxygen delivery and tissue pO_2. Human and bovine Hbs should have the same intrinsic oxygen-carrying capacity because they have the same heme concentration; however, this may be functionally different because of the difference in p50 between Hbs. Studies by Standl *et al.* (29, 30) showed that tissue pO_2 was increased by using PBH in an extreme hemodilution protocol when RBCs were substituted with PBH as an oxygen carrier. These discrepancies can, in part, be ex-

plained by our findings. The initial introduction of PBH in the circulation appears to have a direct effect on microvascular and tissue oxygen metabolism, which is significantly reduced. This reduction is notable because, in some instances (*i.e.*, in our study, and Standl *et al.* (29, 30), tissue pO_2 increased even though oxygen delivery decreased due to vasoconstriction. These effects subside in time. Therefore, analysis of the oxygen-carrying capacity and delivery of HBOCs with characteristics similar to PBH are dependant, to some extent, on the time at which the organism is studied.

In conclusion, these findings indicate that exchange transfusion with PBH to maintain blood oxygen-carrying capacity leads to a significant decrease in oxygen delivery to the microcirculation of the hamster window chamber model. Paradoxically, this effect results in a significant increase in tissue pO_2. Exchange with PBH led to compromised tissue viability evidenced by increased apoptosis, coupled with microcirculatory oxygen imbalance and a significant reduction of tissue oxygen consumption. These effects could be due to changes in mitochondrial oxygen use, oxidative damage and iron saturation. Although decrease in apoptosis and oxygenation imbalance were lowered by treatment with deferoxamine but not eliminated, our results indicate that chelation treatment in cases of large exchange transfusions with molecular Hb solutions is beneficial.

ACKNOWLEDGMENTS

This work has been supported by grants R01-HL76182 to A.G.T., and R24–64395, R01–62354, and R01–62318 to M.I.

DISCLAIMER

Prof. Intaglietta is a member of the Board of the La Jolla Bioengineering Institute.

REFERENCES

1. Alayash AI. Effects of intra- and intermolecular crosslinking on the free radical reactions of bovine hemoglobins. *Free Radic Biol Med* 18: 295–301, 1995.
2. Alayash AI. Oxygen therapeutics: can we tame haemoglobin? *Nat Rev Drug Discov* 3: 152–159, 2004.
3. Balla J, Jacob HS, Balla G, Nath K, Eaton JW, and Vercellotti GM. Endothelial-cell heme uptake from heme proteins: induction of sensitization and desensitization to oxidant damage. *Proc Natl Acad Sci U S A* 90: 9285–9289, 1993.
4. Bates TE, Loesch A, Burnstock G, and Clark JB. Immunocytochemical evidence for a mitochondrially located nitric oxide synthase in brain and liver. *Biochem Biophys Res Commun* 213: 896–900, 1995.
5. Bolanos JP, Almeida A, Stewart V, Peuchen S, Land JM, Clark JB, and Heales SJ. Nitric oxide-mediated mitochondrial damage in the brain: mechanisms and implications for neurodegenerative diseases. *J Neurochem* 68: 2227–2240, 1997.
6. Cabrales P, Sakai H, Tsai AG, Takeoka S, Tsuchida E, and Intaglietta M. Oxygen transport by low and normal oxygen affinity hemoglobin vesicles in extreme hemodilution. *Am J Physiol Heart Circ Physiol* 288: H1885–H1892, 2005.
7. Cheung AT, Jahr JS, Driessen B, Duong PL, Chan MS, Lurie F, Golkaryeh MS, Kullar RK, and Gunther RA. The effects of hemoglobin glutamer-200 (bovine) on the microcirculation in a canine hypovolemia model: a noninvasive computer-assisted intravital microscopy study. *Anesth Analg* 93: 832–838, 2001.
8. D'Agnillo F and Alayash AI. Redox cycling of diaspirin crosslinked hemoglobin induces G_2/M arrest and apoptosis in cultured endothelial cells. *Blood* 98: 3315–3323, 2001.
9. Drugas GT, Paidas CN, Yahanda AM, Ferguson D, and Clemens MG. Conjugated desferoxamine attenuates hepatic microvascular injury following ischemia/reperfusion. *Circ Shock* 34: 278–283, 1991.
10. Endrich B, Asaishi K, Götz A, and Messmer K. Technical report: a new chamber technique for microvascular studies in unanaesthetized hamsters. *Res Exp Med* 177: 125–134, 1980.
11. Fingar VH. Vascular effects of photodynamic therapy. *J Clin Laser Med Surg* 14: 323–328, 1996.
12. Gerald L. *The laboratory hamster.* San Diego: Academic Press, 1987.
13. Guillochon D, Vijayalakshmi MW, Thiam-Sow A, and Thomas D. Effect of glutaraldehyde on hemoglobin: functional aspects and Mossbauer parameters. *Biochem Cell Biol* 64: 29–37, 1986.
14. Halliwell B and Gutteridge JMG. *Free radicals in biology and medicine*. London: Clarendon Press, 1989.
15. Iacovino JR. Evaluation of survival in medically treated patients with homozygous beta thalassemia by the quick hit method. *J Insur Med* 26: 403–404, 1994.
16. Intaglietta M and Tompkins WR. Microvascular measurements by video image shearing and splitting. *Microvasc Res* 5: 309–312, 1973.
17. Kemming GI, Meisner FG, Kleen MS, Meier JM, Tillmans J, Hutter JW, Wojtcyzk C, Packert KB, and Habler OP. Hyperoxic ventilation at the critical hematocrit. *Resuscitation* 56: 285–293, 2003.
18. Kerger H, Groth G, Kalenka A, Vajkoczy P, Tsai AG, and Intaglietta M. pO_2 measurements by phosphorescence quenching: characteristics and applications of an automated system. *Microvasc Res* 65: 32–38, 2003.
19. Lipowsky HH and Zweifach BW. Application of the "two-slit" photometric technique to the measurement of microvascular volumetric flow rates. *Microvasc Res* 15: 93–101, 1978.
20. Manning JE, Katz LM, Brownstein MR, Pearce LB, Gawryl MS, and Baker CC. Bovine hemoglobin-based oxygen carrier (HBOC-201) for resuscitation of uncontrolled, exsanguinating liver injury in swine: Carolina Resuscitation Research Group. *Shock* 13: 152–159, 2000.
21. Moat NE, Evans TE, Quinlan GJ, and Gutteridge JM. Chelatable iron and copper can be released from extracorporeally circulated blood during cardiopulmonary bypass. *FEBS Lett* 328: 103–106, 1993.
22. Morehouse KM, Flitter WD, and Mason RP. The enzymatic oxidation of desferal to a nitroxide free radical. *FEBS Lett* 222: 246–250, 1987.
23. Nagababu E, Ramasamy S, Rifkind JM, Jia Y, and Alayash AI. Site-specific cross-linking of human and bovine hemoglobins differentially alters oxygen binding and redox side reactions producing rhombic heme and heme degradation. *Biochemistry* 41: 7407–7415, 2002.
24. Page TC, Light WR, McKay CB, and Hellums JD. Oxygen transport by erythrocyte/hemoglobin solution mixtures in an in vitro capillary as a model of hemoglobin-based oxygen carrier performance. *Microvasc Res* 55: 54–64, 1998.
25. Pepper JR, Mumby S, and Gutteridge JM. Blood cardioplegia increases plasma iron overload and thiol levels during cardiopulmonary bypass. *Ann Thorac Surg* 60: 1735–1740, 1995.
26. Quinlan GJ, Mumby S, Lamb NJ, Moran LK, Evans TW, and Gutteridge JM. Acute respiratory distress syndrome secondary to cardiopulmonary bypass: do compromised plasma iron-binding antioxidant protection and thiol levels influence outcome? *Crit Care Med* 28: 2271–2276, 2000.
27. Reeder BJ and Wilson MT. Desferrioxamine inhibits production of cytotoxic heme to protein cross-linked myoglobin: a mechanism to protect against oxidative stress without iron chelation. *Chem Res Toxicol* 18: 1004–1011, 2005.
28. Smith RS. Iron excretion in thalassaemia major after administration of chelating agents. *Br Med J* 5319: 1577–1580, 1962.

29. Standl T, Horn P, Wilhelm S, Greim C, Freitag M, Freitag U, Sputteck A, Jacobs E, and Schulte am Esch J. Bovine haemoglobin is more potent than autologous red blood cells in restoring muscular tissue oxygenation after profound isovolaemic haemodilution in dogs. *Can J Anaest* 43: 714–723, 1996.
30. Standl TG, Reeker W, Redmann G, Kochs E, Werner C, and Schulte am Esch J. Haemodynamic changes and skeletal muscle oxygen tension during complete blood exchange with ultrapurified polymerized bovine haemoglobin. *Intensive Care Med* 23: 865–872, 1997.
31. Steward A, Williamson I, Madigan T, Bretnall A, and Hassan IF. An improved animal model for studying desferrioxamine. *Br J Haematol* 95: 654–659, 1996.
32. Torres Filho IP and Intaglietta M. Microvessel pO_2 measurements by phosphorescence decay method. *Am J Physiol* 265: H1434–H1438, 1993.
33. Tsai AG, Friesenecker B, Mazzoni MC, Kerger H, Buerk DG, Johnson PC, and Intaglietta M. Microvascular and tissue oxygen gradients in the rat mesentery. *Proc Nat Acad Sci U S A* 95: 6590–6595, 1998.
34. Tsai AG, Friesenecker B, McCarthy M, Sakai H, and Intaglietta M. Plasma viscosity regulates capillary perfusion during extreme hemodilution in hamster skin fold model. *Am J Physiol* 275: H2170–H2180, 1998.
35. Tsai AG, Johnson PC, and Intaglietta M. Oxygen gradients in the microcirculation. *Physiol Rev* 83: 933–963, 2003.
36. Tsai AG, Vandegriff KD, Intaglietta M, and Winslow RM. Targeted O_2 delivery by low-P50 hemoglobin: a new basis for O_2 therapeutics. *Am J Physiol Heart Circ Physiol* 285: H1411–H1419, 2003.
37. Turner JJ, Rice-Evans CA, Davies MJ, and Newman ES. The formation of free radicals by cardiac myocytes under oxidative stress and the effects of electron-donating drugs. *Biochem J* 277: 833–837, 1991.
38. Winslow RM. Current status of blood substitute research: towards a new paradigm. *J Intern Med* 253: 508–517, 2003.
39. Winterbourn CC. *Reaction of superoxide with hemoglobin: CRC handbook of methods for oxygen radical research.* Boca Raton, Florida: CRC Press, 1985.
40. Yang P, Smith JR, Damodar KS, Planck SR, and Rosenbaum JT. Visualization of cell death in vivo during murine endotoxin-induced uveitis. *Invest Ophthalmol Vis Sci* 44: 1993–1997, 2003.

Address reprint requests to:
Pedro Cabrales
La Jolla Bioengineering Institute
505 Coast Boulevard South.
La Jolla, CA 92037

E-mail: pcabrales@ucsd.edu

Date of first submission to ARS Central, July 7, 2006; date of revised submission, September 13, 2006; date of acceptance, September 18, 2006.

This article has been cited by:

1. Brandon J. Reeder . 2010. The Redox Activity of Hemoglobins: From Physiologic Functions to Pathologic Mechanisms. *Antioxidants & Redox Signaling* **13**:7, 1087-1123. [Abstract] [Full Text HTML] [Full Text PDF] [Full Text PDF with Links]
2. Stefano Bruno, Luca Ronda, Serena Faggiano, Stefano Bettati, Andrea MozzarelliOxygen Delivery via Allosteric Effectors of Hemoglobin and Blood Substitutes . [CrossRef]
3. Pedro Cabrales, Amy G. Tsai, Marcos Intaglietta. 2009. POLYMERIZED BOVINE HEMOGLOBIN CAN IMPROVE SMALL-VOLUME RESUSCITATION FROM HEMORRHAGIC SHOCK IN HAMSTERS. *Shock* **31**:3, 300-307. [CrossRef]
4. Pedro Cabrales, Amy G. Tsai, Marcos Intaglietta. 2008. Balance between vasoconstriction and enhanced oxygen delivery. *Transfusion* **48**:10, 2087-2095. [CrossRef]
5. Pedro Cabrales, Amy G. Tsai, K. Ananda, Seetharama A. Acharya, Marcos Intaglietta. 2008. Volume resuscitation from hemorrhagic shock with albumin and hexaPEGylated human serum albumin. *Resuscitation* **79**:1, 139-146. [CrossRef]
6. SEETHARAMA A. ACHARYA, MARCOS INTAGLIETTA, AMY G. TSAI. 2007. Modulation of the polyethylene glycol-hemoglobin structure to increase the efficiency of plasma expansion and O 2 carrying capacity. *Transfusion Alternatives in Transfusion Medicine* **9**:4, 254-264. [CrossRef]
7. Amy G. Tsai , Paul C. Johnson , Marcos Intaglietta . 2007. Is the Distribution of Tissue pO2 Homogeneous?. *Antioxidants & Redox Signaling* **9**:7, 979-984. [Abstract] [Full Text PDF] [Full Text PDF with Links]